Science Advances

AAAS

advances.sciencemag.org/cgi/content/full/3/6/e1700731/DC1

Supplementary Materials for

Differential intron retention in *Jumonji* chromatin modifier genes is implicated in reptile temperature-dependent sex determination

Ira W. Deveson, Clare E. Holleley, James Blackburn, Jennifer A. Marshall Graves, John S. Mattick, Paul D. Waters, Arthur Georges

Published 14 June 2017, *Sci. Adv.* **3**, e1700731 (2017)
DOI: 10.1126/sciadv.1700731

The PDF file includes:

Other Supplementary Material for this manuscript includes the following:
(available at advances.sciencemag.org/cgi/content/full/3/6/e1700731/DC1)

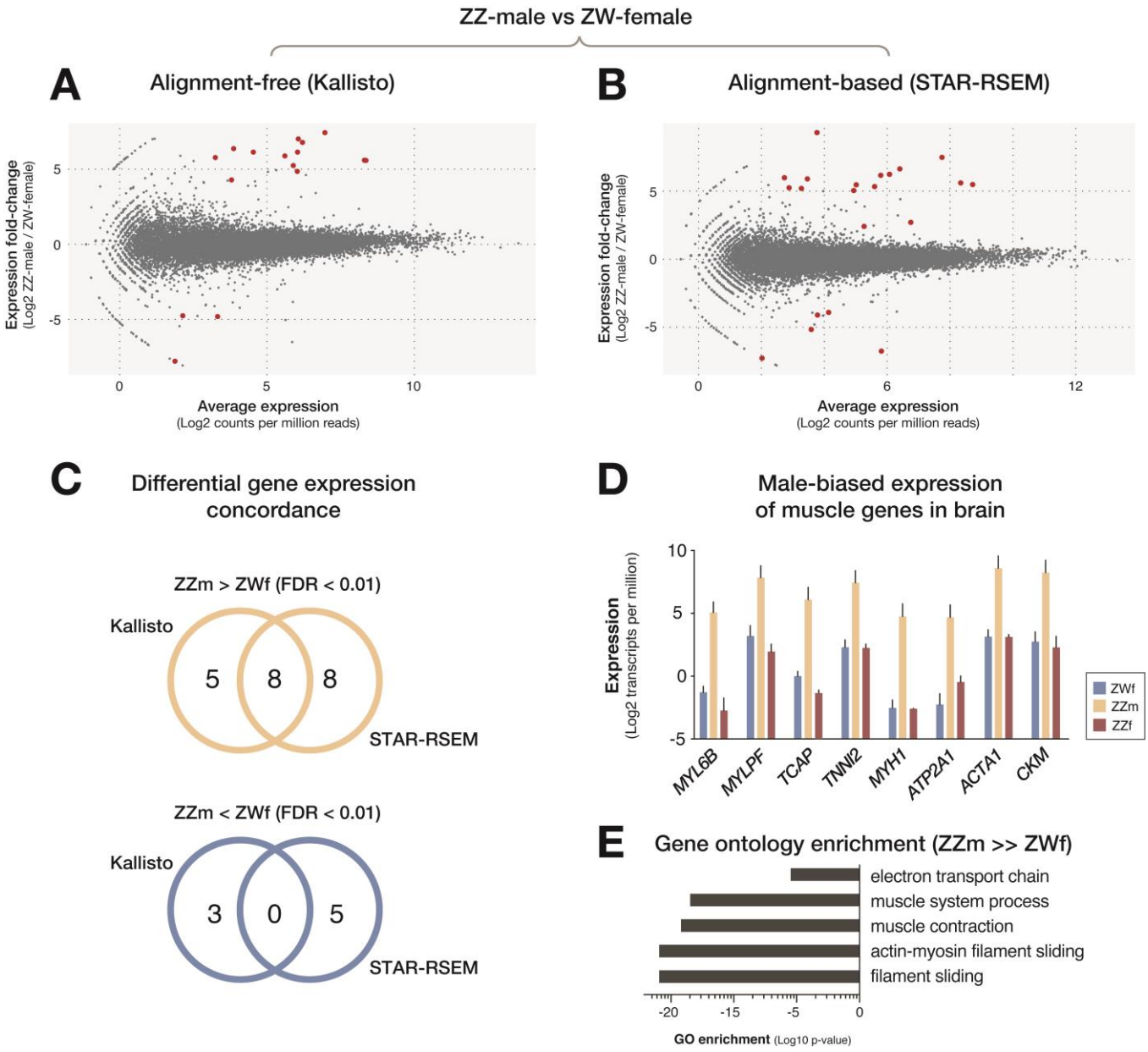

fig. S1. Comparison of gene expression in male and female dragons. Gene expression profiles for normal female (ZWf) and male (ZZm) dragons were compared in order to identify sex-specific differences. (**A** and **B**) Volcano plots show average gene expression fold-change between adult brain from ZZm and ZWf relative to average normalized expression level (mean; *n* = 2). Expression measurements were made separately using Kallisto alignment-free quantification (A) and STAR-RSEM alignment-based quantification (B). Under each method, genes that exceeded a differential expression threshold of FDR < 0.01 are highlighted (red dots). (**C**) Venn diagrams show the number of genes that were found to be differentially expressed (FDR < 0.01) under either or both methods of quantification. Only genes concordant between the two methods were reported as differentially expressed. (**D**) We found eight genes that were significantly over-expressed in ZZm relative to ZWf brain. All eight are involved in canonical muscle processes, including the eminent muscle genes *Actin* (*ACTA1*), *Myosin* (*MYH1*), *Troponin* (*TNNI2*) and *Creatine kinase* (*CKM*). The plot shows the average normalized expression (transcripts per million; mean +/- SD; *n* = 2) recorded in adult brain from

ZWf, ZZm and sex-reversed female (ZZf) dragons for the eight genes that were differentially expressed between ZZm and ZWf. Importantly, ZZf dragons exhibited normal female expression for all sex-biased genes. (**E**) Gene ontology terms that were enriched (GOrilla) among the top 500 genes upregulated in ZZm, relative to ZWf, brains included 'muscle system process' as well as related sub-terms like 'filament sliding' and 'electron transport chain'. Collectively, these data reveal a previously unreported male-bias in the expression of canonical muscle genes in dragon brain.

ZZ-female vs ZW-female

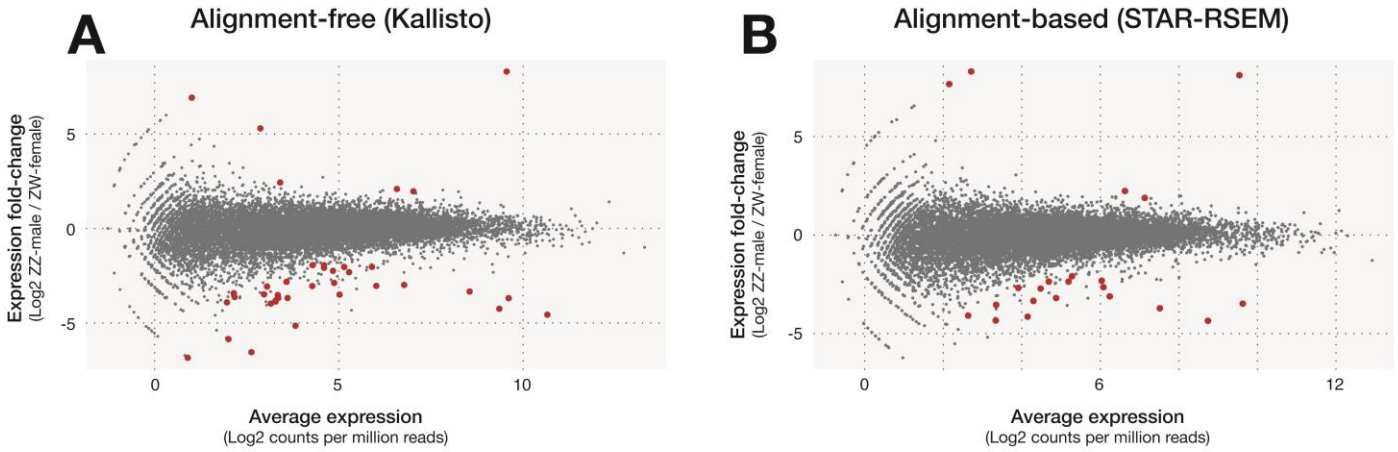

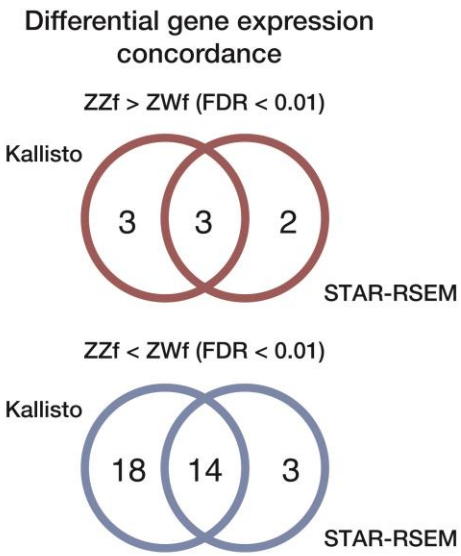

D Concordant differentially expressed genes

Dragon ID	Relative	Log2FC	Predicted ortholog
Pvit_04187	ZZf > ZWf	8.30	Proopiomelanocortin (POMC)
Pvit_04953	ZZf > ZWf	2.09	Circadian associated repressor of transcription (CIART)
Pvit_10415	ZZf > ZWf	1.97	Jumonji AT rich interactive domain 2 (JARID2)
Pvit_19005	ZZf < ZWf	-4.57	Hemaglobin alpha 1
Pvit_15721	ZZf < ZWf	-4.25	Hemaglobin beta
Pvit_15720	ZZf < ZWf	-3.69	Hemaglobin beta
Pvit_16731	ZZf < ZWf	-3.04	Aminolevuliate synthetase 2 (ALAS2)
Pvit_09714	ZZf < ZWf	-3.68	G-protein signalling 18
Pvit_00269	ZZf < ZWf	-3.49	Lysozyme 1 (LYZ1)
Pvit_04860	ZZf < ZWf	-3.68	Parathyroid hormone 2 (PTH2)
Pvit_00442	ZZf < ZWf	-2.04	Pipecolic acid oxidase (PIPOX)
Pvit_14395	ZZf < ZWf	-3.82	Interferon regulatory factor 1 (IRF1)
Pvit_10993	ZZf < ZWf	-3.05	Immunoglobulin heavy chain constant region (IgM)
Pvit_10568	ZZf < ZWf	-2.88	Erythrocyte membrane protein band 4.2 (EPB42)
Pvit_00920	ZZf < ZWf	-2.04	Progestin and adipoQ receptor famil member 6 (PAQR6)
Pvit_14172	ZZf < ZWf	-1.95	Methyltransferase like 10 (METTL10)

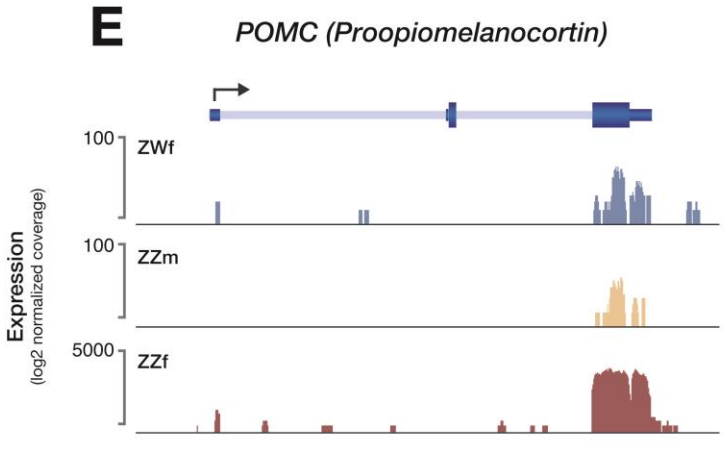

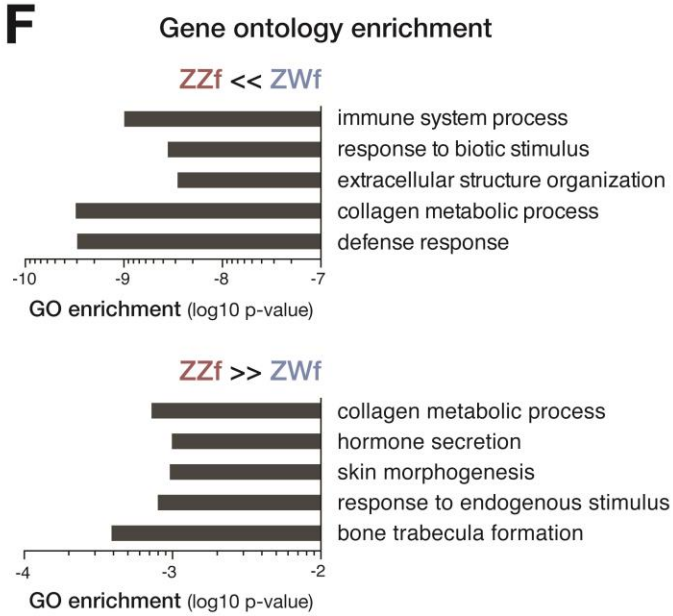

fig. S2. Comparison of gene expression in normal and sex-reversed female dragons. Gene expression profiles of normal female (ZWf) and sex-reversed female (ZZf) dragons were compared in order to identify sex-reversal specific transcriptome features. (**A** and **B**) Volcano plots show average gene expression fold-changes between adult brain from ZZf and ZWf relative to average normalized expression level (mean; *n* = 2). Expression measurements were made separately using Kallisto alignment-free quantification (A) and STAR-RSEM alignment-based quantification (B). Under each method, genes that exceeded a differential expression threshold of FDR < 0.01 are highlighted (red dots). (**C**) Venn diagrams show the number of genes that were found to be differentially expressed (FDR < 0.01) under either or both methods of quantification. Only genes concordant between the two methods were reported as differentially expressed. (**D**) 17 genes were classified as differentially expressed between ZZf and ZWf, of which 14 were down-regulated in ZZf. Expression of prominent immune genes, such as *IgM* and *IRF1,* was reduced in ZZf dragons compared to ZWf or ZZm, while the circadian regulator, *CIART,* was over-expressed. The immune and circadian systems are known to be intertwined with stress. (**E**) Annotated gene model for the predicted ortholog of *Proopiomelanocortin* (*POMC*) in dragon. Normalized coverage by mapped RNA sequencing reads shows expression of *POMC* in a single replicate of ZWf (blue), ZZm (yellow) and ZZf brain (red). (**F**) Top 5 non-redundant gene ontology terms (GOrilla) that were enriched among the top 500 genes down-regulated (above) or up-regulated (below) in ZZf, relative to ZWf, individuals.

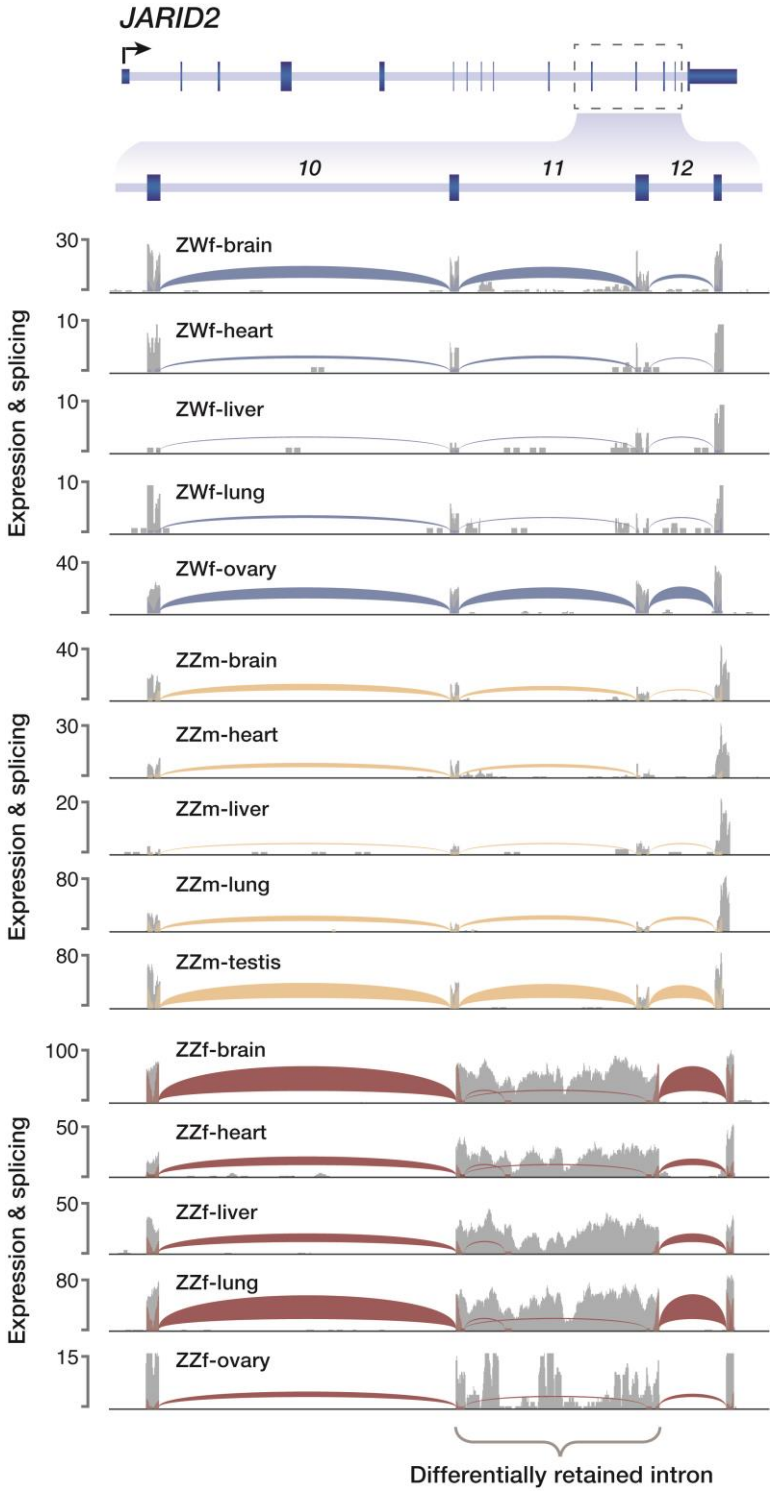

fig. S3. Differential *JARID2* IR in normal and sex-reversed dragons. Annotated gene model for the predicted ortholog of *JARID2* in dragon. Normalized coverage by mapped RNA sequencing reads (gray) and density of spliced-read junctions (colored) spanning annotated introns are shown for a single replicate from adult tissues for normal female (ZWf; blue), male (ZZm; yellow) and sex-reversed female (ZZf; red).

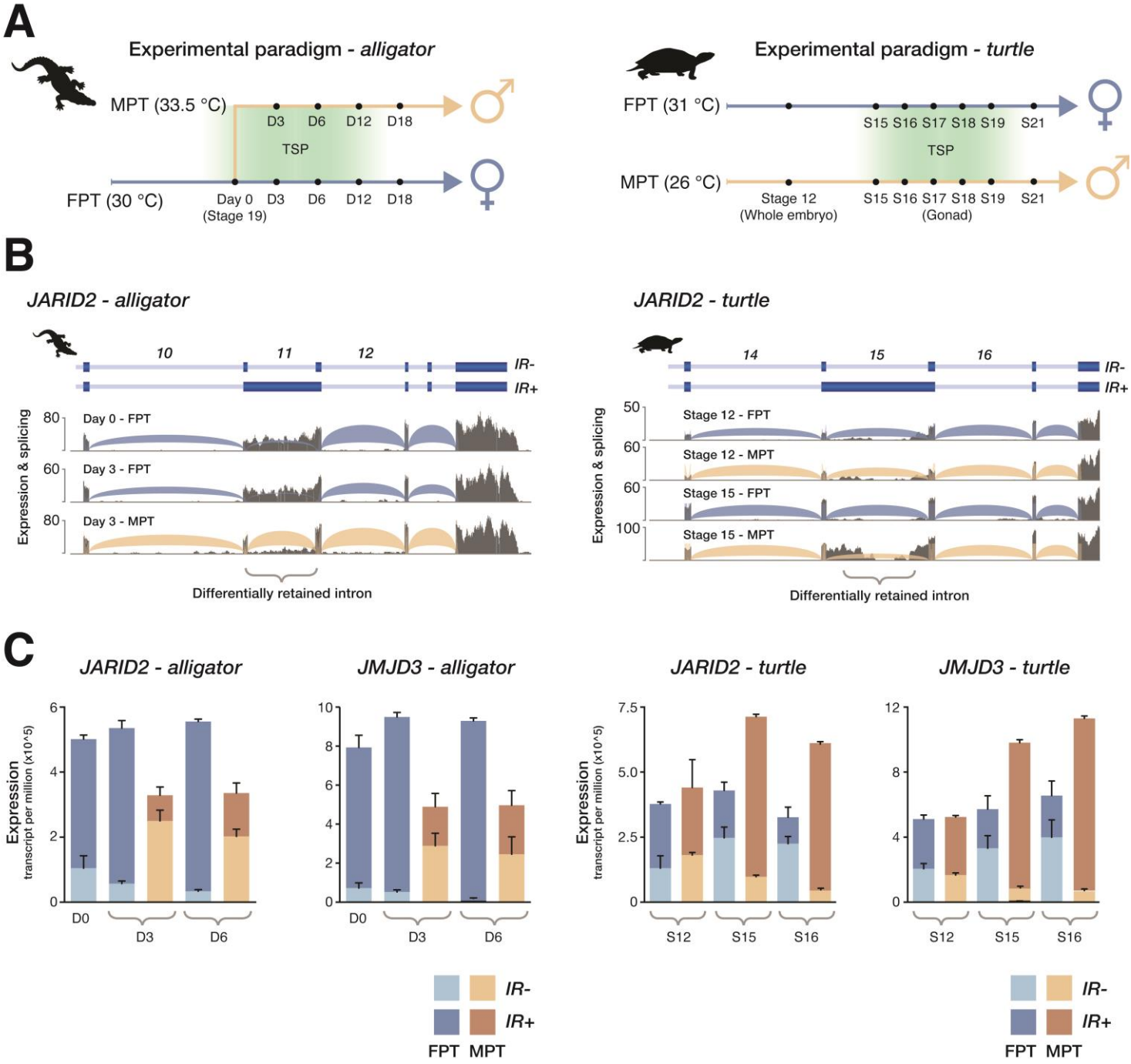
A
Experimental paradigm - alligator
MPT (33.5 °C)
D3 D6 D12 D18
TSP
FPT (30 °C)
Day 0 D3 D6 D12 D18
(Stage 19)
Experimental paradigm - turtle
FPT (31 °C)
S15 S16 S17 S18 S19 S21
TSP
MPT (26 °C)
Stage 12
(Whole embryo)
S15 S16 S17 S18 S19 S21
(Gonad)
B
JARID2 - alligator
10 11 12
IR-
IR+
Expression & splicing
Day 0 - FPT
Day 3 - FPT
Day 3 - MPT
Differentially retained intron
JARID2 - turtle
14 15 16
IR-
IR+
Expression & splicing
Stage 12 - FPT
Stage 12 - MPT
Stage 15 - FPT
Stage 15 - MPT
Differentially retained intron
C
JARID2 - alligator
JMJD3 - alligator
JARID2 - turtle
JMJD3 - turtle
Expression
transcript per million (x10^5)
D0 D3 D6
S12 S15 S16
IR-
IR+
FPT MPT

fig. S4. Temporal dynamics of *JARID2/JMJD3* expression and splicing in alligator and turtle embryo. (**A**) Alligator eggs were incubated under FPT (30°C) until Ferguson developmental stage 19, a period in which the gonads are still bipotential and morphologically indistinguishable. At stage 19, a subset of eggs was shifted to MPT (33.5°C) while the remaining eggs were maintained at FPT for the subsequent incubation period. Tissues comprising the developing gonad were sampled at FPT of day 0, then at FPT and MPT at multiple time points after stage 19. Full procedure is described in reference (4). Turtle eggs were separately incubated at FPT (31°C) or MPT (26°C) from the day of laying. Whole embryos were sampled at FPT and MPT at development stage 12, before the initiation of gonad development. Gonads were then sampled at FPT and MPT from stage 15-21, fully encompassing the temperature sensitive period of development. Full procedure is described in reference (5). (**B**) Normalized coverage by mapped RNA sequencing reads (gray) and density of spliced read junctions spanning annotated introns are shown for a single replicate of: (left) alligator embryonic gonad at FPT day 0 (stage 19; blue), FPT day 3 (blue) and MPT day 3 (yellow); (right) turtle whole stage 12 embryos at FPT (blue) and MPT (yellow) and embryonic gonad at stage 15 FPT (blue) and MPT (yellow). Note that the section of zero-coverage in the center of the retained intron for turtle is a string of undefined (N) bases in the genome, to which reads cannot be mapped. (**C**) Average normalized expression (transcripts per million; mean +/- SD; n = 3) for spliced (IR-) and intron retaining (IR+) isoforms of *JARID2* and *JMJD3* in alligator and turtle. Measurements shown are from alligator gonad at FPT day 0 and FPT/MPT day 3 and 6 and turtle FPT/MPT whole stage 12 embryos, and embryonic gonads at FPT/MPT stage 15 and 16.

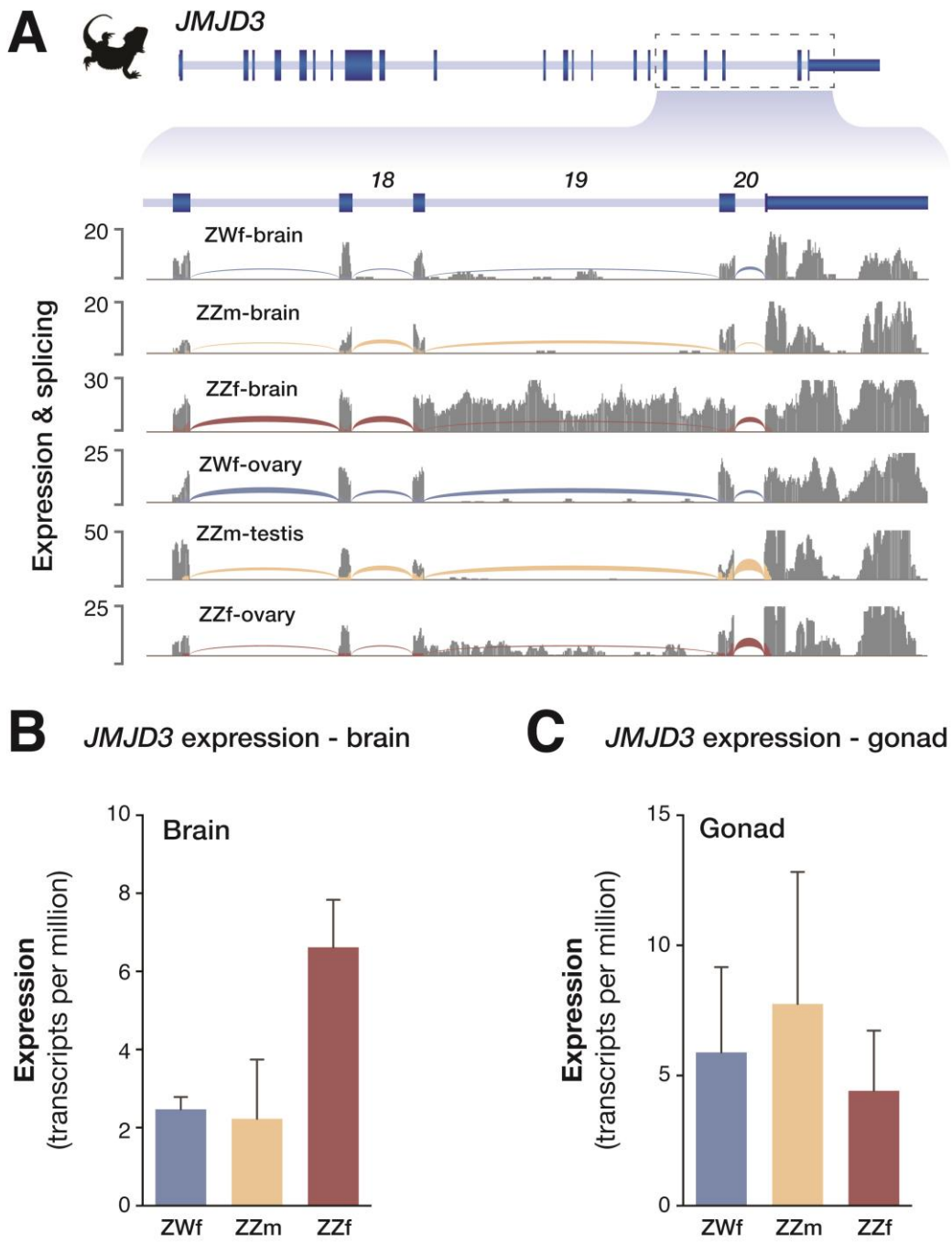

fig. S5. Expression and splicing of *JMJD3* in the brain and gonad from normal and sex-reversed dragons. (**A**) Annotated gene model for the predicted ortholog of *JMJD3* in dragon. Normalized coverage by mapped RNA sequencing reads (gray) and density of spliced read junctions (colored) spanning annotated introns are shown for for a single replicate from adult brain for normal female (ZWf; blue), male (ZZm; yellow) and sex-reversed female (ZZf; red). (**B** to **C**) Average normalized expression of *JMJD3* (transcripts per million; mean +/- SD; n = 2) recorded in adult brain (B) and gonad (C) from ZWf, ZZm and ZZf individuals.

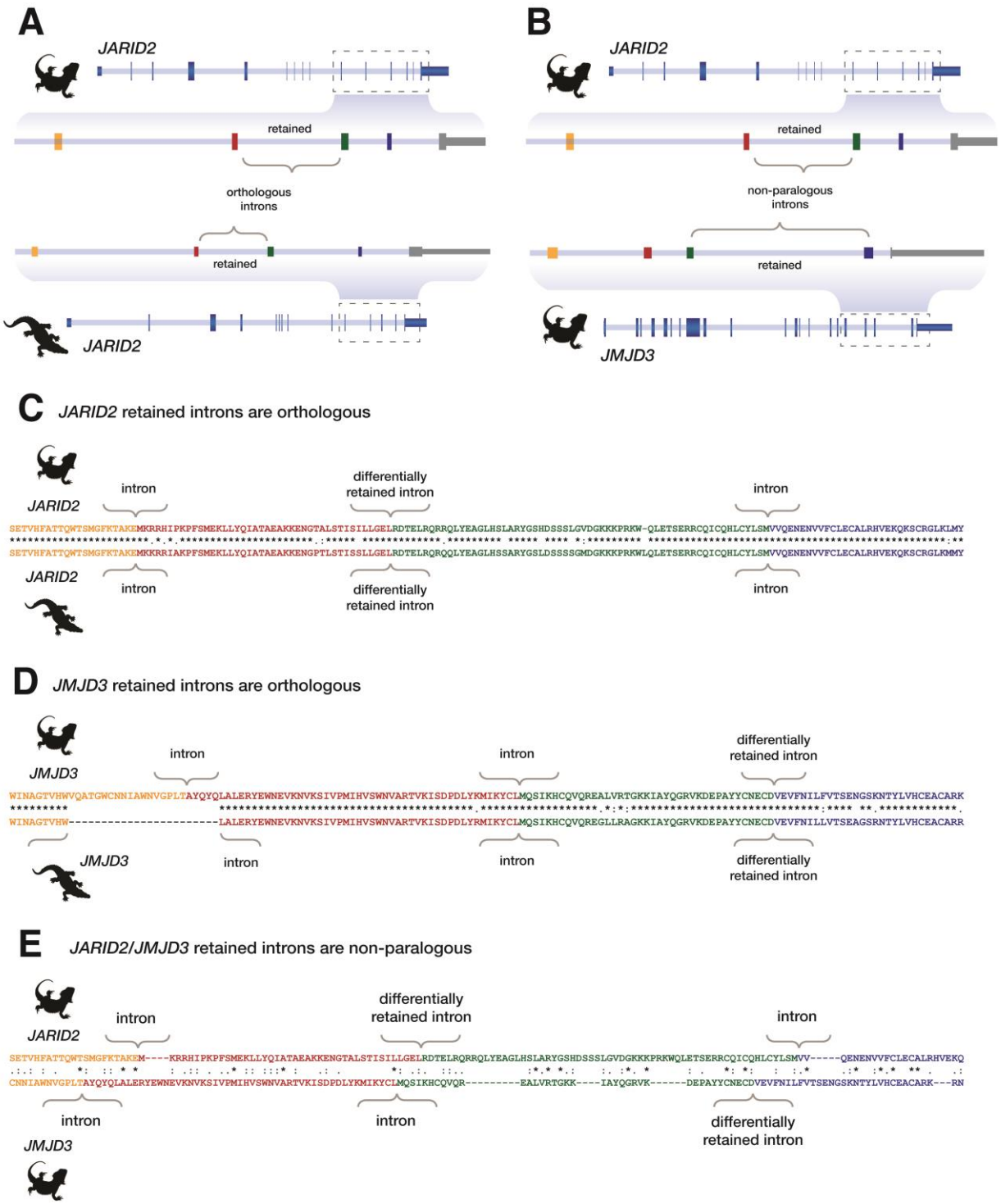

fig. S6. Differentially retained introns in *JARID2/JMJD3* are nonparalogous. (**A** to **B**) This schematic shows the relationship between orthologous introns, which fall between ortholgous coding exons, and non-paralogous introns, which do not fall between paralogous coding exons. (**C** to **E**) Alignment (MUSLCE) of peptide sequences for dragon and aligator *JARID2* (C), dragon and aligator *JMJD3* (D) and dragon *JARID2/JMJD3* (E), with exon-intron architecture indicated. Alignments demonstrate that the differentially retained introns identified in dragon and alligator *for JARID2/JARID2* and *JMJD3/JMJD3* are orthologous but the differentially retained introns in *JARID2/JMJD3* are not paralagous to one and other, suggesting that their capacity for differential retention is not underpinned by a shared conserved sequence element. The same relationships were true for *JARID2/JMJD3* differentially retained introns between dragon/turtle and alligator/turtle (not shown).